

6. Preclinical Studies

6.1 Introduction

The major aspect considered after design and optimization of any delivery system is to establish its therapeutic efficacy, safety profile, potential to deliver the therapeutics preferably to the site of action and estimate the dosage regimen. Pharmacokinetics plays a pivotal role in drug designing, screening and formulation development process as it gives complete information about absorption, distribution, metabolism and excretion (ADME characters) of the molecules. Pre-clinical studies on rodents help in identifying a lead molecule, screening of suitable formulation, determination of administration route, selection of dosage regimen and also in estimating the dose for phase I clinical trials [1,2]. Pharmacokinetic studies also help in evaluation of new or novel delivery systems, level of selective distribution or other changes of pharmacokinetic profile of novel delivery. The better therapeutic efficacy of nanoparticulate delivery systems is due to altered pharmacokinetic profile in the body as well as ability to reach target site. Change of pharmacokinetic characters of any drug delivery systems including novel drug designing can direct prospect of attaining better therapeutic efficacy. Hence, pharmacokinetics and bio-distribution studies of the developed novel drug delivery systems are crucial [3,4]. The biological performance of any nanocarrier systems depends on several parameters like particle size, size distribution, morphology, shape, surface potential and also surface chemistry of particles [5,6]. To estimate the changes in the *in vivo* behavior of nanoparticulate systems and to estimate their safety and efficacy, pharmacokinetic studies were conducted. Surface modifications of the nanoparticulate systems lead to a significant change in pharmacokinetic and biodistribution parameters [5–8]. Moreover, efficacy assessment for the designed nano-formulations were studied in Alzheimer induced rat model [9–12]. In the present study polymeric nanoparticles of donepezil (DNP) have been developed with the objective to enhance brain delivery. The concentration of DNP in plasma and other organs was estimated for free drug and developed polymeric nanoparticles. The pharmacokinetic and biodistribution parameters of the nano-formulations were evaluated and compared with the free drug to evaluate and understand the effect of nano-formulations on the pharmacokinetics and distribution to the brain. Further, efficacy studies were performed in the developed Alzheimer's animal model.

6.2 Experimental

6.2.1 Materials

Drug, formulation excipients and chemicals were obtained from same source as discussed in chapter 5. All surgical instruments like scissors, forceps, blades and needles were sterilized before use. A β ₁₋₄₂ peptide, 5,5'-dithiobis-(2-nitrobenzoic acid) (DTNB), xylazine, ketamine, sodium dodecyl sulphate (SDS), ascorbic acid and thiobarbituric acid (TBA) were procured from Sigma-Aldrich, USA. TNF- α and IL-6 ELISA kits were purchased from Ray Biotech Inc. BDNF ELISA kit was procured from Boster Biological Tech. Ltd, USA. A β ₁₋₄₂ and pTau ELISA kits were acquired from Elab Science.

6.2.2 Equipment's

- Spectrophotometer: UV-1800 Shimadzu, Japan
- Elisa Plate reader: Epoch microplate spectrophotometer, Biotek, Winooski, US
- Tissue Homogeniser: Kinematica™ Polytron™ Homogenizers, Germany
- Digital Microscope: Zeiss Microscopes, Jena, Germany
- Stereotaxic Instrument: Inco Ambala, India
- Hamilton syringe: Sigma Aldrich, USA
- Anymaze Video tracking system: Stoelting Co., USA
- Actophotometer: Inco Ambala, India
- Passive Avoidance Task: Inco Ambala, India

6.2.3 Animals

All experimental animals (Wistar rats; either sex; 8–10 weeks; weighing around 200–220 g) were purchased from Central Animal Facility, Department of Pharmacy, BITS-Pilani, Pilani campus, India. Animals were placed in polyacrylic cages and kept under controlled conditions (12 h light/dark cycle, 22 \pm 1°C with relative humidity of 60%). Animals were nourished with normal pellet diet and purified water *ad libitum* throughout the acclimatization and study period. All procedures involving sample collection, isolation of tissues, surgical process and their care were performed as per IAEC guidelines of BITS-Pilani, Pilani campus, India (protocol numbers: IAEC/RES/22/05 and IAEC/RES/22/05/Rev-1/23/25). Moreover, all the behavioral studies were performed in day time in between 09.00 to 17.00 h only and while performing behavioral evaluation studies animal cages were placed in the analysis room 0.5 h before starting analysis to

allow habituation. None of the behavioral analysis was completed during any single day cycle. During analysis animals were cleaned if required as per protocols.

6.3 Pharmacokinetic studies

Animals were randomly divided into five different groups (each group consists of 4 animals) viz. free drug dissolved in 0.9% saline, D1-NPs, D2-NPs and D3-NPs were administered orally at a dose of 5 mg/kg. Additionally, one more group of free drug with an intravenous administration was performed at a same dose. Blood samples were collected in heparinized polypropylene disposable tubes from the retro-orbital plexus at pre-determined time intervals. Plasma was obtained by centrifuging the blood samples at 6000 rpm for 15 min and stored at -80 ± 10 °C until analysis.

The plasma samples were analyzed by an in-house developed and validated HPLC method by using loratadine as an internal standard with solid phase extraction technique as discussed in chapter 3. Pharmacokinetic parameters were estimated by using compartmental and non-compartmental analysis. Selection of model was decided by visual inspection method, Akaike's information (AIC) criterion, Schwarz information criterion (SBC) and coefficient of regression. The lowest AIC and SBC value suggests best fit model [13]. Various pharmacokinetic parameters like concentration maximum (C_{max}), area under curve (AUC_{0-inf}), mean residence time (MRT), volume of distribution in central compartment (V_1), volume of distribution in peripheral compartment (V_2), plasmatic clearance (Cl), intercompartmental clearance (CLD_2), alpha half-life ($t_{1/2 \alpha}$), beta half-life ($t_{1/2 \beta}$), and elimination rate constants of two compartmental model (K_{10}, K_{12}, K_{21}) were estimated Phoenix WinNolin Certera™ (Pharsight, U.S.A; version:8.0) [14].

6.4 *In vitro-in vivo* correlation (IVIVC)

The IVIVC was estimated by utilizing Level-A correlation to build a correlation among *in vitro* dissolution and *in vivo* plasma drug concentration of D1-NPs, D2-NPs and D3-NPs. The model independent approach viz. numerical deconvolution was performed [15]. The numerical deconvolution involved the utility of a weighing fraction, unit impulse response (UIR) for which pharmacokinetics of single i.v. bolus dose of free drug was employed. Regression analysis data was utilized to validate the correlation among the fraction of *in vivo* drug release and *in vitro* drug absorbed. Analysis was executed using Phoenix WinNonlin 8.0 with an add-on IVIVC toolkit (Certara™, U.S.A.) software. As per FDA guidelines, the mean absolute percent prediction error (% PE) for the predicted C_{max} and AUC should not exceed more than 15% [16].

6.5 Biodistribution studies

To investigate the biodistribution of free drug, D1-NPs, D2-NPs and D3-NPs were administered to Wistar rats orally at a dose of 5 mg/kg respectively (18 rats per each group). Animals were anaesthetized and sacrificed at 0.25, 0.5, 1, 4, 12, 24 h (three rats/time point) by cervical dislocation. All the organs (brain, heart, lungs, kidney, spleen and liver) were collected promptly and rinsed thoroughly with ice-cold saline to remove any blood or other components and blotted with filter paper. An accurately weighed quantity of each tissue samples were homogenized in 1:2 w/v of phosphate buffer saline solution by using tissue homogenizer. After homogenization, centrifugation was done at 10000 rpm for 15 min, clear supernatant was collected and stored at -80°C until analysis [14,17].

6.6 Pharmacodynamic studies

Based on the results obtained from bio-distribution studies we have selected D3-NPs further to conduct pharmacodynamic studies.

6.6.1 Administration of intracerebroventricular (ICV) - A β ₁₋₄₂ peptide

All the surgical experiments were performed in Wistar rats (200-220 g). Prior to the stereotaxic surgery, rats were anaesthetized using an intraperitoneal injection of ketamine–xylazine mixture (80 mg/kg and 5 mg/kg respectively). The skull of the rat was opened by a midline sagittal incision over the scalp after placing the head of the rat in exact location of the stereotaxic apparatus. Further, two holes were drilled through the skull into the lateral cerebral ventricles utilizing the previously reported coordinates as 0.8 mm posterior to bregma, 1.5 mm adjacent to sagittal suture and 3.6 mm ventral over the surface of the brain [18–21]. Antiseptic powder (Neosporin) was administered after surgery to prevent from sepsis. A β ₁₋₄₂ peptide solution was prepared as discussed in chapter 4 and diluted with citrate buffer (pH 4.4). A freshly prepared sample of A β ₁₋₄₂ peptide was administered at a nominal dose of 5 μ M/kg.

6.6.2 Standardization of ICV administration

The ICV administration was standardized and confirmed by drilling through the skull as per the co-ordinates reported earlier [18,20,21]. Instead of A β ₁₋₄₂ peptide administration, a dye solution was infused in the ICV region by using Hamilton syringe. Further, the animal was sacrificed and the brain sections were observed after 30 min storage at -20 °C. As represented in Fig. 6.1, it clearly

shows the accumulation of dye solution in the lateral ventricular regions. Thus, the ICV administration to the specific selected co-ordinates was optimized.

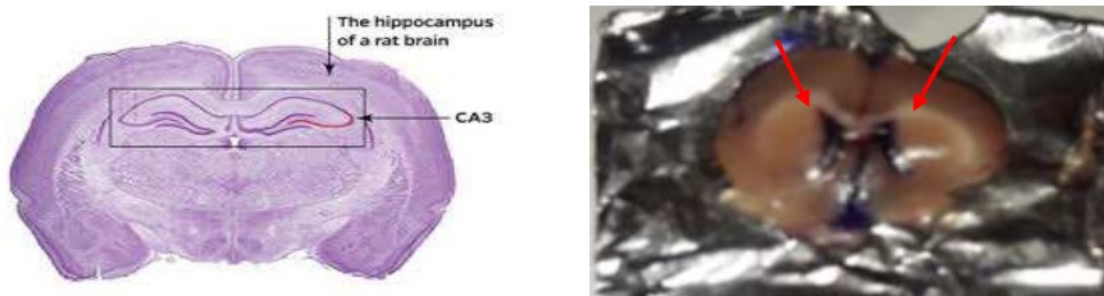


Fig. 6.1 Standardization of intracerebroventricular administration

6.6.3 Experimental schedule

Animals were divided into four different groups (10 animals per group). The experimental schedule and evaluation intervals of different parameters were represented in Fig. 6.2.

Group 1: Sham control, rats were administered with citrate buffer by ICV route at a volume of 5 μ L in each ventricle on day 1.

Group 2: Rats were infused with ICV- $A\beta_{1-42}$ solution at a volume of 5 μ L in each ventricle on day 1.

Group 3: Rats were administered with free drug (5 mg/kg; p.o.), after the $A\beta_{1-42}$ administration starting from day 1 and continued once daily for a period of 21 days.

Group 4: Rats were administered with D3-NPs (5 mg/kg; p.o.), after the $A\beta_{1-42}$ administration starting from day 1 and continued once daily for a period of 21 days.

Design of Treatment Schedule

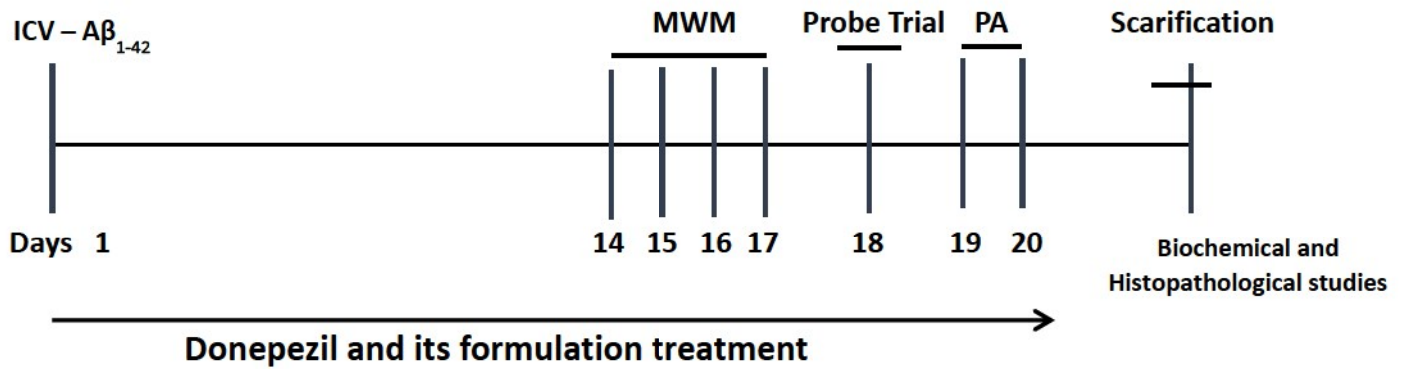


Fig. 6.2 Experimental schedule for treatment and the intervals for determination of various parameters in ICV-Aβ₁₋₄₂ induced cognitive deficits. ICV-Aβ₁₋₄₂ = Intracerebroventricular-Aβ₁₋₄₂; MWM = Morris water maze; PA= Passive avoidance

6.6.4 Behavioral assessment for cognitive function

(a) Morris water maze (MWM)

Rationale: For studying spatial learning and memory in animals one of the most widely explored behavioral test is MWM analysis. During experimentation, all the animals learn to swim in a water tank, directed by external signs and to climb up a submerged platform. The animals the pathway to find the platform, based upon spatial learning information. Moreover, rats and mice are the natural swimmers, but during this task they will try to get out of the water. This experiment is simple yet powerful maze design which can be used in behavioral analysis to estimate cognitive function, examine animal models of neurodegenerative disorders and efficacy estimation of potential drugs or formulations [22–25].

Procedure: In our study, a circular water tank with the dimensions of 120 cm diameter and 60 cm height was selected for performing MWM analysis. The tank was filled with water (27 ± 1 °C) till a depth of 40 cm and was further separated into four quadrants like south-west, south-east, north-west and north-east. In one of the selected quadrants, a hidden platform (10 cm x 5 cm) was positioned 2 cm beneath the water surface and it has been located in the same spot during the entire experimentation. Prior to start training, animals were permitted to swim freely in the tank for about 60 s by removing the hidden platform. Further, animals were provided training having a ceiling time of about 60 s containing of four trials per each analysis (once from each quadrant) for four

days. Once the animals climb onto the hidden platform, they are allowed to remain there itself for 30 s before beginning of next session. Although, if the animal is unable to reach the platform in the experimental time of 60 s, it was located over the hidden platform and permitted to stay here for the same time interval. Moreover, the time required to identify the hidden platform was recorded as latency in seconds by utilizing ANY-maze video tracking device (Stoelting Co. USA) [26–28].

(b) Probe trial

A probe trail was performed to estimate the reference memory at the end of learning. After 24 h animals were exposed to a probe trial individually as it is the last navigation trial in MWM. In the probe trial, next to the removal of hidden platform each animal was released from one of the quadrants and is permitted to freely swim for 60 s. Further, time spent in the specific quadrant by each animal where the platform was placed in the training session was considered as measurement for spatial memory in probe trial [25,27,29].

(c) Passive avoidance task

Rationale: In order to learn and avoid an aversive stimulus, passive avoidance task is performed and the training may be once or multi-trials. There is a punishment to a rodent in the experimental process with an electric footshock, thus it is an aversive task.

Procedure: The experimental procedure was performed as per previously reported methods [30]. In brief, the device consists of two chambers; one is illuminated and the other one is dark chamber. However, they were divided by a guillotine door and have a shock scrambler grid floor in both the chambers. In the acquisition trial, each animal was positioned in the illuminated chamber and later 60 s the separating door was unlocked. The time spent to enter the dark compartment was recorded as initial latency and if any animal takes above 60 s it was excepted for further procedure. Once the animal enters the dark chamber the separating door was locked and supplied an electrical foot shock with a capacity of 50 V over the grid floor for about three seconds. Retention latency was determined after 24 h in the similar manner, but the electrical foot shock was not applied and the latency time was measured up to 300 s. Short retention latency time indicates lesser retention memory. The apparatus was properly cleaned and dried in between trails with dilute (70 % v/v) alcohol.

6.6.5 Behavioral assessment for motor function

(a) Spontaneous locomotor activity

Animals were assessed for spontaneous locomotor activity as per the previously reported methods [30,31]. Briefly, each animal was placed in a square closed arena with dimensions 30 x 30 cm consisted of infrared light sensitive photocells for a period of 10 min by utilizing a digital actophotometer (INCO, India) to estimate the spontaneous locomotor function. In between each trial, the apparatus was cleaned and dried with 70% v/v ethanol.

6.6.6 Biochemical parameters

All the biochemical estimates were quantified in the hippocampus homogenate sample obtained after euthanizing the animals as per the approved protocol.

(a) Hippocampus homogenate preparation

Animals were euthanized and the brain samples were promptly harvested. The hippocampus region of the brain was separated and homogenized in 1:10 w/v of chilled saline by utilizing tissue homogenizer [14]. Followed by, centrifugation at 10000 rpm for 15 min at 4 °C, supernatant was obtained and analyzed for biochemical parameters.

(b) Protein determination

The amount of protein quantity in brain homogenates was estimated by the reported method utilizing BSA (1mg/mL) as a standard [32].

(c) Quantification of acetylcholinesterase (AChE) activity

Cholinesterase inhibitors (ChEIs) enhances the breakdown of AChE in synaptic cleft, thus enhancing ACh levels. The estimation of AChE activity in brain samples were performed as per methods reported earlier [30,33]. In brief, the assay sample contained 50 µL of brain homogenate, 100 µL of acetylthiocholine iodide, 3 mL of 0.01 M sodium phosphate buffer (pH 8) and 100 µL of DTNB (Ellman reagent). The samples were immediately quantified at a wavelength of 412 nm by utilizing UV-visible spectrophotometer. Results were estimated by molar extinction constant ($1.36 \times 10^4 \text{ M}^{-1} \text{ cm}^{-1}$) and represented as nanomoles per milligram of protein.

(d) Quantification of malondialdehyde (MDA) level

The end product of lipid peroxidation is MDA which was determined by using TBA as per the reported methods [34,35]. Briefly, the assay sample contained 100 µL of brain homogenate, 750 µL of 20% glacial acetic acid (pH: 3.5), 100 µL of 8 % SDS, 750 µL of 0.8 % TBA and 300 µL of purified water. Further the mixture of this sample was heated up to 95 °C for about 1 h and the

supernatant was obtained by centrifugation at 10,000 rpm for 10 min. In the obtained supernatant solution, the amount of MDA was quantified at 532 nm by using Epoch microplate spectrophotometer (Biotek, Winooski, USA). The standard curve was plotted in brain homogenate using tetramethoxypropane and the data was expressed as nanomoles of MDA per milligram protein.

(e) Quantification of reduced glutathione (GSH) level

The glutathione levels in the brain homogenate samples was quantified by using Ellman method [36]. In brief, same volumes of 5% sulphosalicylic acid and brain homogenate sample was mixed and stored at 4 °C for about 1h. Supernatant was attained by centrifugation at 10,000 rpm for 10 min at 4 °C and from this 50 µL of the sample was mixed with 350 µL of phosphate saline buffer (pH: 7.4) and 1.5 mL of 4% DTNB. This mixture was incubated at 37 °C for 10 min and analyzed at 412 nm by using Epoch microplate spectrophotometer (Biotek, Winooski, USA). Standard curve was plotted in brain homogenate utilizing glutathione and the data was represented as micromoles of GSH per milligram protein [30,37].

(f) Quantification of nitrite level

The deposition of nitrite levels is a hallmark for nitric oxide production which was quantified by calorimetric assay using Greiss reagent as reported earlier [38,39]. In brief, equal volumes of brain homogenate supernatant solution and Greiss reagent were mixed and incubated for about 10 min at a room temperature and the data was recorded at an absorbance of 540 nm using Epoch microplate spectrophotometer (Biotek, Winooski, USA). Standard curve was plotted using sodium nitrite in brain homogenate and the data was represented as micromoles of nitrite per milligram protein.

(g) Quantification of superoxide dismutase (SOD) level

The levels of SOD in the brain homogenates was determined by previously reported methods [40,41]. In brief, 100 µL of sample was mixed with 800 µL of 0.37 % glycine and 20 µL of epinephrine. Further this mixture was incubated at 37 °C for 5 min. and quantified at 480 nm using Epoch microplate spectrophotometer (Biotek, Winooski, USA). The data was expressed as micromoles of SOD per milligram protein.

(h) Quantification of pro-inflammatory cytokines

In the rat hippocampus homogenate samples, the level of pro-inflammatory cytokines TNF- α and IL-6 were measured by utilizing a commercially accessible ELISA kit as per the manufacturer's protocol (Ray Biotech Inc. ELR-TNFA-1 and ELR-IL6-1).

(i) Quantification of brain derived neurotrophic factor (BDNF) level

BDNF levels in the rat hippocampus homogenate was quantified using ELISA kit and the procedure was followed as per the manufacturer's instructions (Boster Biological Tech. Ltd, EK0308).

(j) Quantification of A β ₁₋₄₂ level

A β ₁₋₄₂ level in the rat hippocampus homogenates were estimated by utilizing a commercially accessible A β ₁₋₄₂ ELISA kit as per manufacturer's protocol (Elab Science, E-EL-M0068).

(k) Quantification of phosphorylated tau (p-tau) level

In the rat hippocampus homogenate samples, the level of p-tau was measured using a commercially accessible ELISA kit according to the manufacturer's protocol (Elab Science, E-EL-M1121).

(l) Histopathological studies

The brain samples were immediately harvested and fixed by using 10% formalin solution. Then samples were prepared by embedding it in paraffin wax and stained with H & E after sectioning them into 5 μ m thick sections. Hippocampal dentate gyrus (DG) and cornu ammonis (CA1) area of the samples were studied using Zeiss microscope at 100x and 400x. By using ImageJ software, the number of deteriorating neurons were counted and expressed in percentage [42]. Neurons with visible cytoplasm, round shape and single large nucleolus were measured as healthy neurons and was represented with yellow arrows. Whereas, neurons with irregular shape and shrinkage with dark stained nuclei were identified as a degenerating or pyknotic neurons and was represented with red arrows.

6.7 Statistical analysis

The data is expressed as mean \pm standard deviation (SD) and all experiments were independently repeated at least three times. Statistical analysis was assessed using one-way analysis of variance (ANOVA) followed by tukey's post hoc multiple comparison tests calculated using GraphPad prism (v 6.0), *p* values <0.05.

6.8 Results and Discussion

6.8.1 Pharmacokinetic studies

The pharmacokinetic studies for free drug, D1-NPs, D2-NPs and D3-NPs were performed in wistar rats. As per i.v bolus administration of free drug, a bi-exponential decline was observed in the log plasma drug concentration vs time plot (Fig. 6.3), hence data was fitted in two-compartmental model [14]. Mean \pm SD plasma drug concentration versus time profiles for DNP solution and all the nanoparticles are shown in Fig. 6.4. After oral administration of DNP and its formulations, all at a dose of 5mg/kg, obtained plasma drug profiles suggested improvement in pharmacokinetic characters of nanoparticulate systems. The drug was absorbed quickly from all the NPs and peak drug concentration reached in less than 1 h (t_{max}), as in case of pure drug (Table 6.1). All NP formulations produced higher peak concentration (C_{max}), nearly double to that of pure drug indicating better absorption from all the nanoformulations. Compared to pure drug, in all the formulations, DNP plasma concentrations were found to be much higher and for longer duration. In pure drug the concentration became very low in 24 h but for NPs it continued for more than 72 h with best for D3-NPs, indicating higher residence time. These results suggest that biodistribution of drug from NPs changed and more drug is remaining in blood with slower elimination. Elimination of all the NPs were found to enhanced from 4 to 7 times with D3-NPs exhibited maximum of 7-fold ($p < 0.05$) increase in plasma elimination half-life ($t_{1/2\beta}$) than DNP solution. The $AUC_{0-\infty}$ were found to be much higher for all the NPs but maximum for D3-NPs (16532.19 ± 776.54 ng.h/ml) in comparison to free drug which indicated the long circulating ability of the formulation in plasma. The clearance (Cl) was found to decreased many folds for all NPs with of D3-NPs showed ~ 13.38 fold ($p < 0.05$) decrease than free drug. These change in profile is due to less ability of NPs to distribute to other parts of body and thus remained longer in blood. Influence of these changes in pharmacokinetic characters on selective and better distribution to brain is discussed later (section 6.8.3)

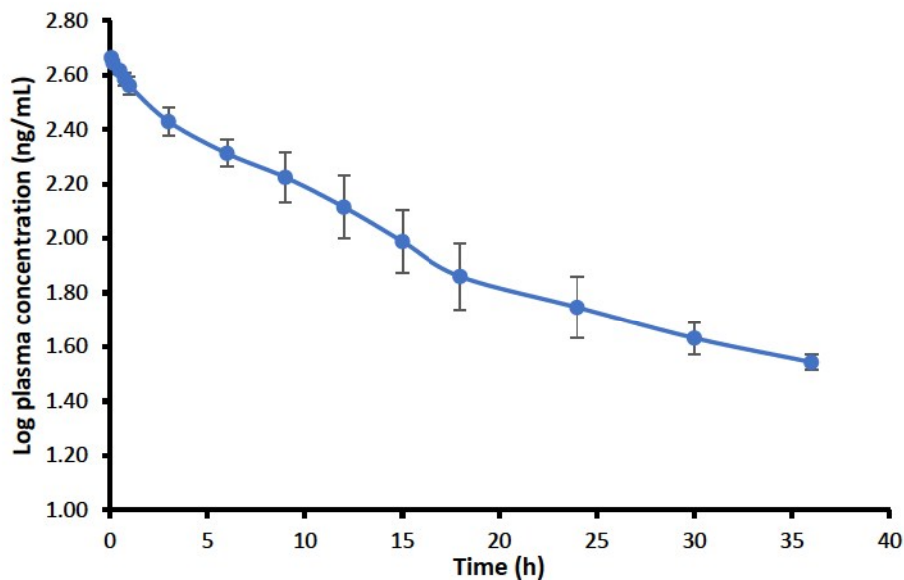


Fig. 6.3 Log plasma drug concentration versus time plot after i.v. bolus administration

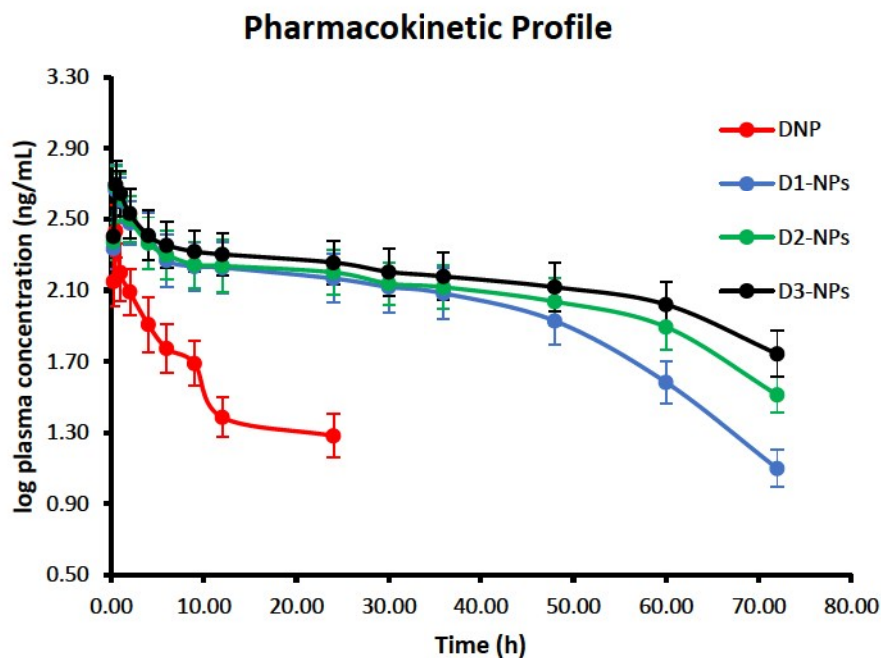


Fig.6.4 Plasma concentration-time profile for DNP and its formulations (mean \pm SD, n=4)

Table 6.1: Pharmacokinetic parameters of DNP after p.o. (5mg/kg) administration in rats

Parameter	Units	Free drug	D1-NPs	D2-NPs	D3-NPs
T _{max}	h	0.48 \pm 0.01	0.70 \pm 0.03	0.69 \pm 0.02	0.69 \pm 0.02
C _{max}	ng/mL	237.76 \pm 56.18	446.46 \pm 89.15	466.16 \pm 72.29	484.61 \pm 86.49
T _{1/2β}	h	6.30 \pm 0.91	28.83 \pm 2.19	39.39 \pm 3.48	44.79 \pm 3.18
K ₀₁	1/h	2.69 \pm 0.06	2.42 \pm 0.09	2.84 \pm 0.05	2.99 \pm 0.15

K ₁₀	1/h	0.43 ± 0.01	0.08 ± 0.01	0.06 ± 0.01	0.04 ± 0.01
K ₁₂	1/h	1.50 ± 0.32	0.87 ± 0.19	0.67 ± 0.09	0.63 ± 0.06
K ₂₁	1/h	0.63 ± 0.04	0.42 ± 0.05	0.33 ± 0.04	0.36 ± 0.03
AUC _{0-∞}	h*ng/mL	1235.57 ± 298.48	10203.48 ± 315.15	13097.33 ± 395.14	16532.19 ± 386.12
CL	mL/h/kg	4046.71 ± 198.15	490.03 ± 95.11	381.76 ± 86.28	302.44 ± 54.48

6.8.2 *In vitro in-vivo* correlation

Level-A (IVIVC) model was developed using the drug dissolution and *in vivo* data [15]. The IVIVC profile is essential for dosage form development and also for quality control point of view. IVIVC plot displaying correlation between plasma concentration (ng/mL) and fraction bioavailability versus time (h) of the formulations were determined (Fig. 6.5). Further, statistical parameters percent prediction errors for C_{max} and AUC were within the limits with a fold error less than 10 for the selected internal validation formulation (Table 6.2).

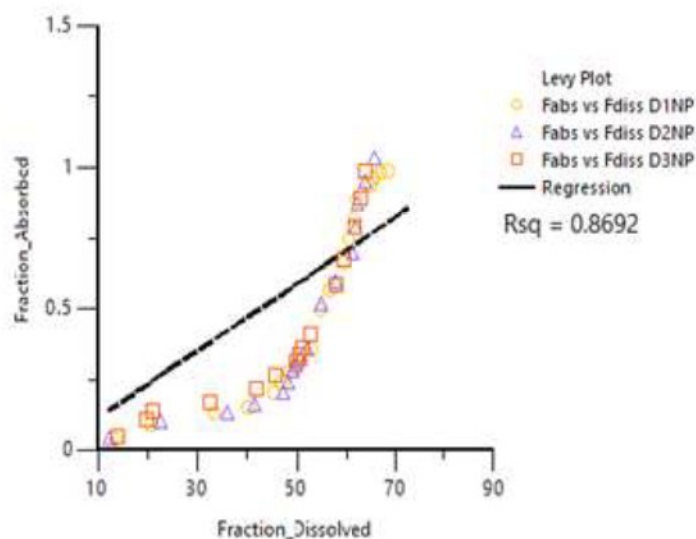


Fig. 6.5 Fraction dissolved versus fraction absorbed correlation graph generated by Phoenix software

Table 6.2: IVIVC internal validation correlation

Parameter	Predicted	Observed	% PE
C _{max}	437.76	484.61	- 9.61
AUC	14980.87	16532.19	- 9.38

6.8.3 Biodistribution studies

Biodistribution studies were performed to identify the potential nano-formulation for the brain targeting efficiency after oral administration. DNP distribution pattern was quantified in all the major organs. The concentration time profiles of brain and liver are represented in Fig.6.6. In brain the concentration levels of pure drug was observed for 4 h only but for all the NPs it continued for more than 24 h. D3-NPs exhibited ~5.8 fold ($p < 0.05$) increase in the brain uptake and ~15.30 fold ($p < 0.05$) decrease in brain clearance rate (Cl) than that of pure drug (Table 6.3). Moreover D1-NPs and D2-NPs also exhibited similar trend but the highest brain uptake was observed in D3-NPs which might be due to the presence of ApoE3 lipoprotein carrier. DNP has been reported for hepatotoxicity due to excess accumulation in liver, the same trend has been noticed in case of pure drug. Interestingly, all the NPs displayed a significant decrease in the accumulation of DNP in liver it might be due to presence of polycaprolactone moiety and targeting moieties attached over the surface of nanoparticles [15]. The $AUC_{0-\infty}$ for D3-NPs was found to be 5274.35 ± 777.26 h.ng/mL which is ~2.89 fold ($p < 0.05$) lower than pure drug (15241.01 ± 929.48 h.ng/mL).

For all the NPs, the concentration of DNP in kidney was lower than that of pure drug, indicating the higher clearance rate. D3-NPs exhibited ~2.31 fold ($p < 0.05$) greater than pure drug. Further, in case of lungs and heart the concentration levels were initially lower for all the NPs but after 24 h a slight increment was observed than pure drug. In spleen the concentration levels were maintained for longer duration at a lower clearance rate in comparison with pure drug. The pharmacokinetic parameters for the other tissues were tabulated in Table 6.4.

Additionally, D3-NPs has strong affinity with LDL-R, it binds specifically to these receptors and enters brain due to presence of ApoE3 coating. Apart from this, ApoE3 has antioxidant and antiamyloidogenic activity which helps in rapid amyloid beta clearance [43]. Thus, these results suggested that, D3-NPs exhibited selective distribution to the brain due to surface modifications. Hence, it may reduce the side effects associated with DNP. Moreover, these finding of the biodistribution studies were in complementary relation to the systemic pharmacokinetic data as well as cellular uptake studies.

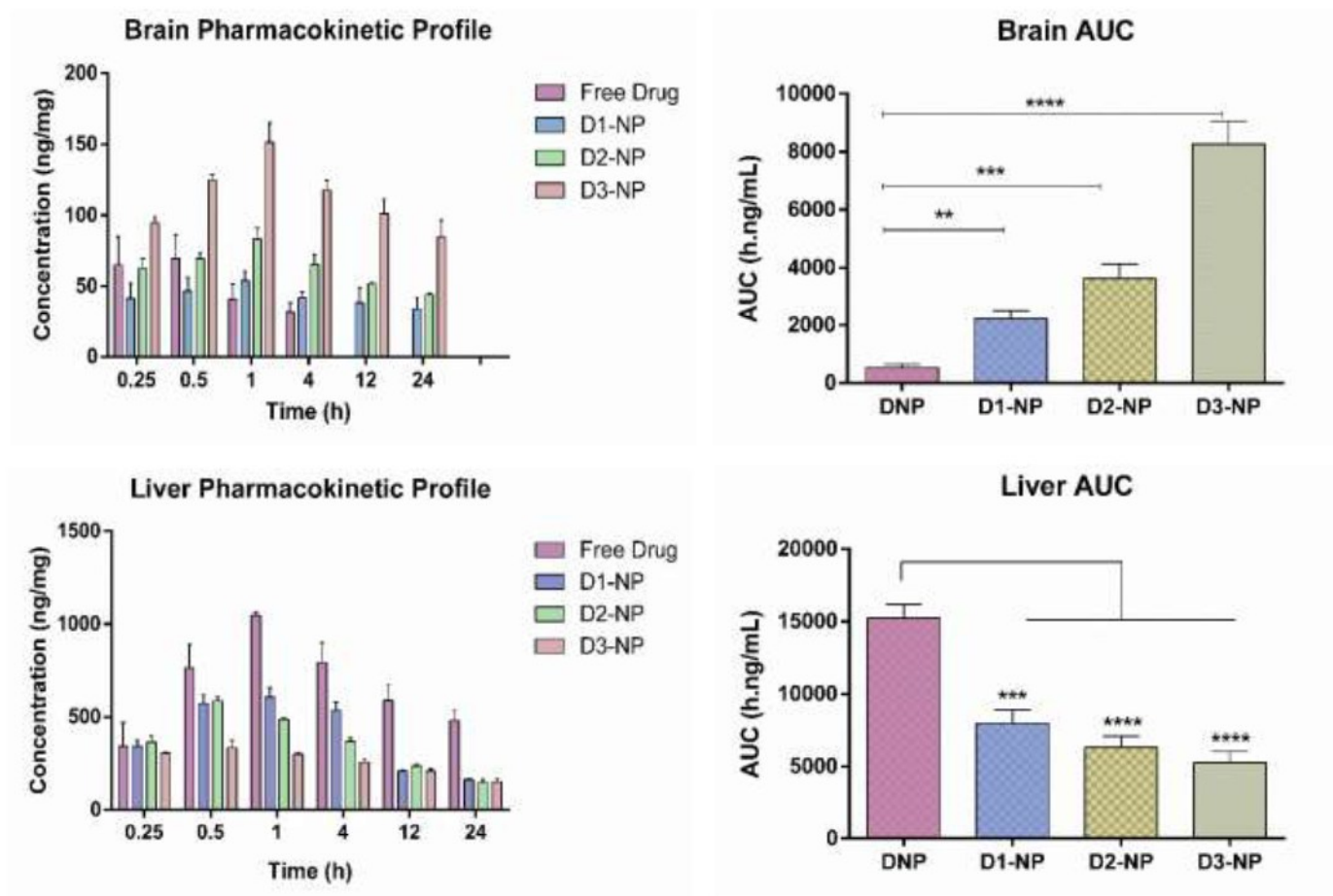


Fig.6.6 Brain and liver concentration-time profile for DNP and its formulations (mean \pm SD, n=3), * indicates $p < 0.05$, when compared with free drug

Table 6.3: Brain pharmacokinetic parameters of DNP after per oral (5mg/kg) administration in rats

Parameters	Units	Free drug	D1-NPs	D2-NPs	D3-NPs
Tmax	h	0.50 ± 0.00	1.00 ± 0.00	1.00 ± 0.00	1.00 ± 0.00
Cmax	ng/mg	69.82 ± 16.35	53.90 ± 21.59	83.34 ± 26.94	151.51 ± 34.18
MRT	h	11.72 ± 2.98	40.42 ± 7.26	52.20 ± 9.54	67.54 ± 8.66
AUC _{0-∞}	h*ng/mL	541.01 ± 86.45	2226.63 ± 136.59	3629.89 ± 269.89	8274.35 ± 298.45
CL	mL/h/kg	9241.91 ± 120.69	2245.54 ± 109.85	1377.45 ± 70.98	604.28 ± 55.32

Table 6.4: Other tissues pharmacokinetic parameters of DNP after per oral (5mg/kg) administration in rats

Parameters	Tmax (h)			Cmax (ng/mg)			MRT (h)			AUC _{0-∞} (h.ng/mL)			CL (mL/h/kg)			
	Free Drug	D1-NPs	D2-NPs	D1-NPs	D2-NPs	D3-NPs	Free Drug	D1-NPs	D2-NPs	D1-NPs	D2-NPs	D3-NPs	Free Drug	D1-NPs	D2-NPs	D3-NPs
Liver	1.00 ± 0.00	1.00 ± 0.00	0.50 ± 0.00	607.71 ± 1046.19	586.29 ± 334.70	334.70 ± 41.24	41.24 ± 18.45	21.95 ± 38.23	7986.63 ± 15241.01	6329.89 ± 5274.35	496.16 ± 26.87	520.63 ± 37.88	143.11 ± 5.93	496.16 ± 26.87	520.63 ± 37.88	456.84 ± 30.74
	0.50 ± 0.00	0.50 ± 0.00	0.50 ± 0.00	477.41 ± 550.17	500.35 ± 27.62	515.61 ± 30.50	17.00 ± 5.27	32.05 ± 8.04	4986.33 ± 6698.04	5317.93 ± 6478.43	609.88 ± 32.27	498.40 ± 35.02	571.49 ± 22.87	609.88 ± 32.27	498.40 ± 35.02	303.68 ± 29.24
	0.00 ± 0.00	0.00 ± 0.00	0.00 ± 0.00	45.02 ± 55.27	27.62 ± 30.50	30.50 ± 5.27	8.99 ± 5.18	7.62 ± 5.48	533.49 ± 427.71	424.07 ± 516.11	32.27 ± 32.27	35.02 ± 35.02	22.87 ± 22.87	32.27 ± 32.27	35.02 ± 35.02	29.24 ± 29.24
Heart	0.50 ± 0.00	0.50 ± 0.00	0.50 ± 0.00	210.66 ± 296.03	171.08 ± 225.64	225.64 ± 11.44	11.44 ± 4.08	29.25 ± 30.31	1810.68 ± 1751.39	1924.95 ± 1965.32	171.99 ± 29.75	142.28 ± 18.42	248.80 ± 39.32	171.99 ± 29.75	142.28 ± 18.42	138.24 ± 21.21
	0.00 ± 0.00	0.00 ± 0.00	0.00 ± 0.00	38.25 ± 41.15	33.93 ± 32.85	32.85 ± 4.08	4.08 ± 5.18	5.61 ± 5.48	561.15 ± 659.91	659.91 ± 661.25	29.75 ± 29.75	18.42 ± 18.42	39.32 ± 39.32	29.75 ± 29.75	18.42 ± 18.42	21.21 ± 21.21
	0.00 ± 0.00	0.00 ± 0.00	0.00 ± 0.00	48.71 ± 59.61	55.81 ± 41.23	41.23 ± 3.69	3.69 ± 4.62	4.77 ± 4.77	242.59 ± 357.89	345.87 ± 243.95	262.83 ± 262.83	262.83 ± 262.83	26.45 ± 26.45	262.83 ± 262.83	262.83 ± 262.83	215.64 ± 215.64
Kidney	1.00 ± 0.00	1.00 ± 0.00	0.50 ± 0.00	256.62 ± 456.30	241.87 ± 211.42	211.42 ± 21.81	21.81 ± 3.69	33.05 ± 17.96	2785.23 ± 6859.47	3519.29 ± 3293.95	1344.86 ± 729.08	729.08 ± 88.68	488.63 ± 26.45	1344.86 ± 729.08	729.08 ± 88.68	1128.66 ± 1128.66
	0.50 ± 0.00	0.50 ± 0.00	0.50 ± 0.00	290.45 ± 232.02	276.91 ± 293.90	293.90 ± 9.20	9.20 ± 2.62	28.21 ± 5.39	3357.18 ± 908.88	3379.43 ± 3745.99	953.27 ± 1038.54	1038.54 ± 765.16	4404.59 ± 99.85	953.27 ± 1038.54	1038.54 ± 765.16	765.16 ± 765.16
	0.00 ± 0.00	0.00 ± 0.00	0.00 ± 0.00	52.37 ± 44.62	42.32 ± 37.41	37.41 ± 2.62	2.62 ± 5.48	5.39 ± 5.39	278.92 ± 263.41	471.64 ± 398.31	235.24 ± 307.51	307.51 ± 170.35	263.41 ± 263.41	235.24 ± 307.51	307.51 ± 170.35	170.35 ± 170.35

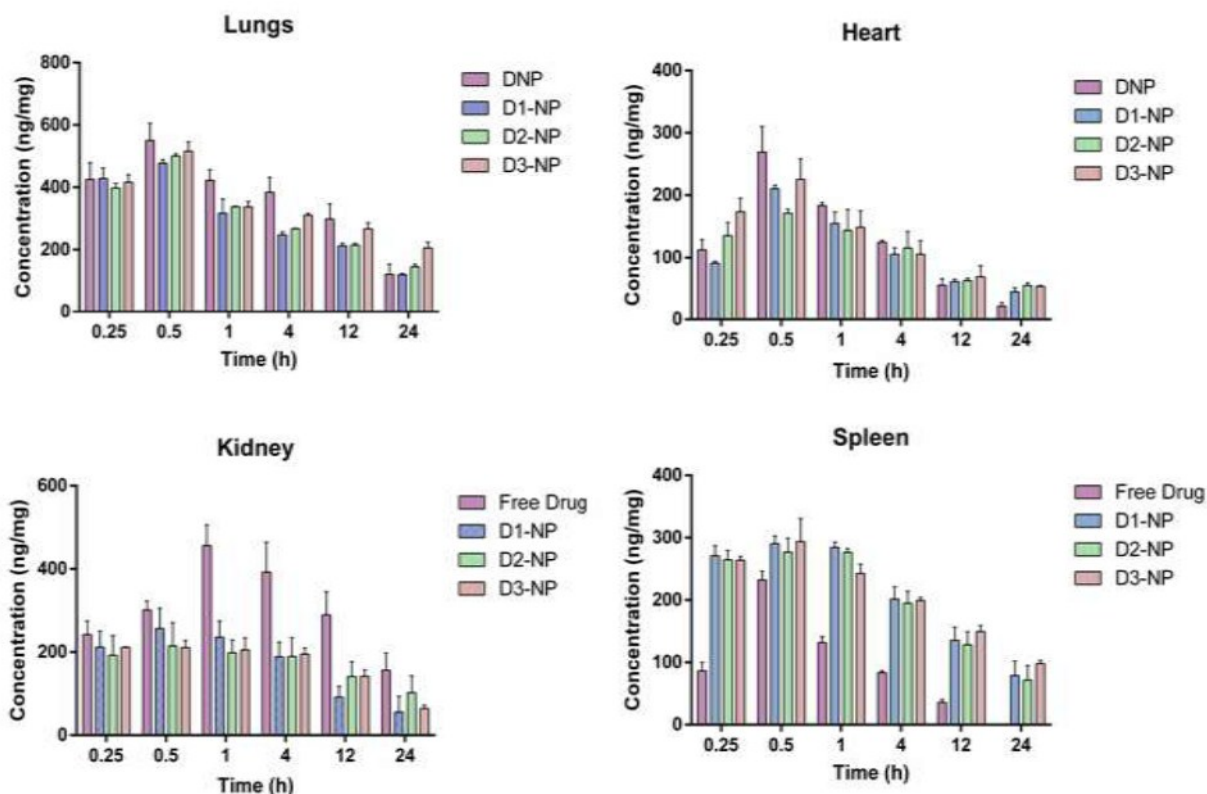


Fig.6.7 Tissue concentration-time profile for DNP and its formulations (mean \pm SD, n=3)

6.8.4 Pharmacodynamic studies

(A) Behavioral assessment for cognitive function

Single behavior analysis in animals may not be able to cover entire aspects of memory and learning. Hence, we have performed a battery of behavioral parameters like MWM and passive avoidance task. Since the introduction of MWM in 1984 it has been widely reported in rodents for behavioral analysis [44]. From the passive avoidance task, short-term memory impairment was estimated.

(i) Morris water maze (MWM)

In all the groups after four days of training session in MWM analysis, gradual reduction in the mean escape latency was detected. However, in case of ICV- $A\beta_{1-42}$ group mean escape latency was significantly higher in comparison with control group. After treatment with free drug and D3-NPs decrease in the escape latency was noticed yet D3-NPs significantly attenuated the effect as shown in Fig. 6.8.

(ii) Probe trial

Hidden platform was removed in case of probe trial, ICV- $A\beta_{1-42}$ injected rats were unsuccessful to recognize the exact place of the platform and spent short period in the particular quadrant than sham control group. When ICV- $A\beta_{1-42}$ injected rats treated with free drug and D3-NPs were capable to remember the precise position of the platform quadrant. Moreover, D3-NPs group spent more time in the platform quadrant than the free drug group, which shows the improvement of memory (Fig. 6.8). These results represent that, D3-NPs were able to attenuate the cognitive deficits induced by $A\beta_{1-42}$ in rats.

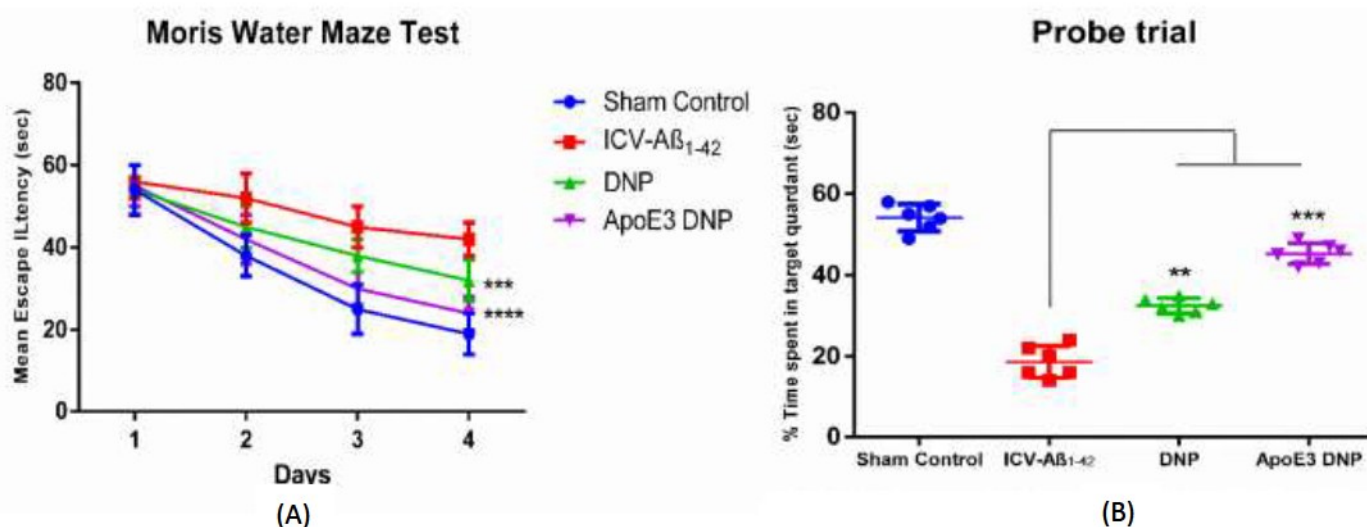


Fig.6.8 Effect of DNP and its formulation on (A) Morris water maze task and (B) probe trial, * indicates $p < 0.05$, when compared with disease control

(iii) Passive avoidance task

There was no significant difference observed in all the experimental groups during the latency time of acquisition trial. But, in case of retention latency a significant decrease in ICV- $A\beta_{1-42}$ group and received electric shocks in comparison with sham group. However decreased retention latency was attenuated in ICV- $A\beta_{1-42}$ group when treated with free drug and D3-NPs indicating improvement in the retention memory and escaped from electric shock. In D3-NPs treated group the retention memory was even higher than that of free drug alone, indicating the efficacy of the formulation with improved consolidation of memory (Fig. 6.9).

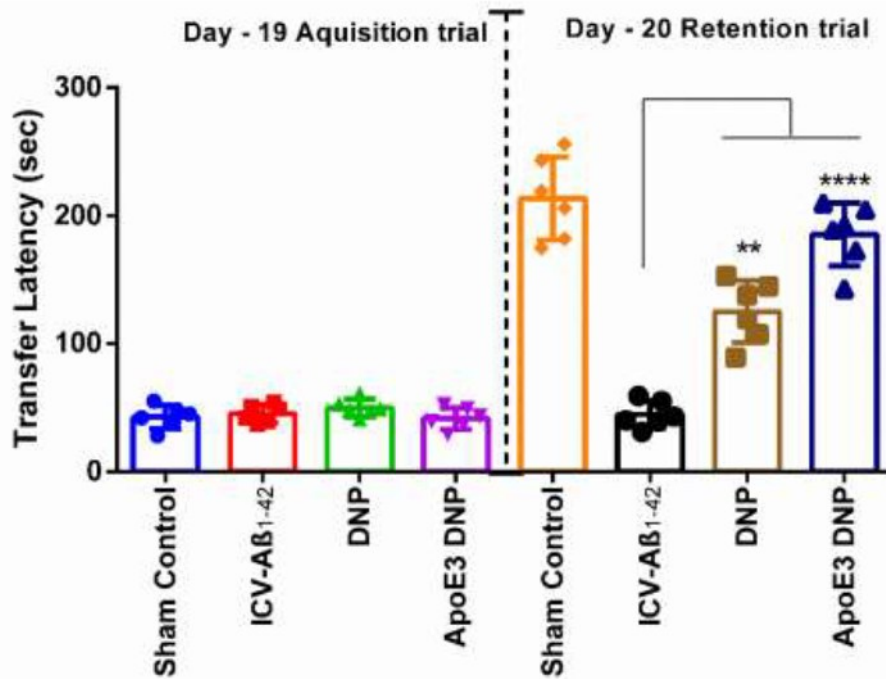


Fig.6.9 Effect of DNP and its formulation in passive avoidance task, * indicates $p < 0.05$, when compared with disease control

(B) Behavioral assessment for motor function

(i) Spontaneous locomotor activity

Spontaneous locomotor activity was carried out to exclude the motor abnormalities in cognitive function estimation. The data represents there was no significant difference among the groups (Fig. 6.10). Moreover, to strengthen the above results and to get insight into the cognitive behavior, biochemical parameters were performed.

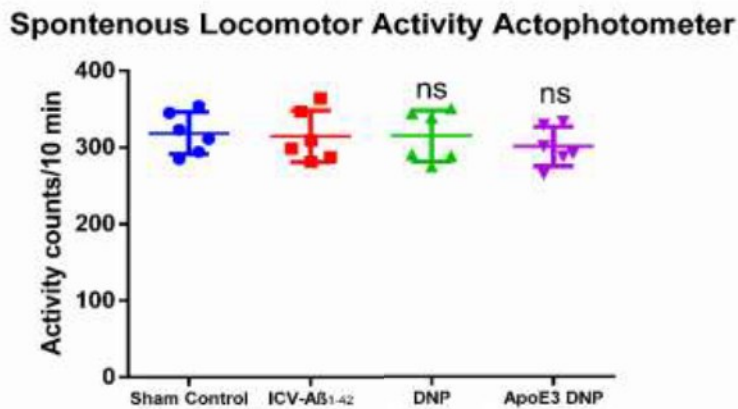


Fig.6.10 Effect of DNP and its formulation on spontaneous locomotor activity, ns indicates $p < 0.05$, when compared with disease control

(C) Biochemical parameters

(i) Estimation of acetylcholinesterase (AChE) activity

Increased level of AChE was observed in the brain homogenates of ICV- $A\beta_{1-42}$ infused group than the sham control group. However, ICV- $A\beta_{1-42}$ group on treatment with DNP and D3-NPs the AChE levels were restored. Further, D3-NPs significantly attenuated AChE activity in comparison with free drug (Fig. 6.11).

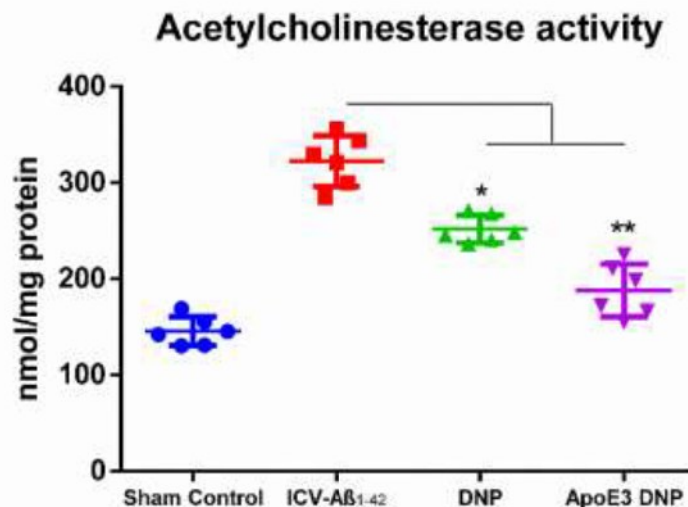


Fig.6.11 Effect of DNP and its formulation on acetylcholinesterase activity, * indicates $p < 0.05$, when compared with disease control

(ii) Estimation of MDA, GSH, nitrite and SOD levels

Elevation in the levels of ROS generation (oxidative stress) and neuroinflammation is one of the major molecular mechanism which is involved in ICV- $A\beta_{1-42}$ induced neurodegeneration. The most susceptible parts of the brain which undergoes impairment in oxidative stress conditions were hippocampus and neocortex regions. To estimate the role of nanoparticles efficacy over $A\beta_{1-42}$ induced oxidative stress, we have determined the level of anti-oxidants (GSH and SOD) and oxidative markers (MDA and nitrite). Results showed that ICV- $A\beta_{1-42}$ group significantly improved the levels of oxidative markers and decreased the levels of endogenous anti-oxidants as represented in Fig. 6.12. Treatment with DNP and D3-NPS, decreased levels of oxidative markers were observed. Moreover, D3-NPs resulted in significant attenuation of oxidative markers (MDA and nitrite) in comparison to free drug alone. The level of anti-oxidants (GSH and SOD) was found to be significantly depleted in ICV- $A\beta_{1-42}$ group than the sham control. When treatment of ICV-

$A\beta_{1-42}$ group with DNP and D3-NPs, it prevented the fall of the defensive enzymes GSH and SOD. D3-NPs exhibited more consistent restoration of these enzyme levels than the free drug alone.

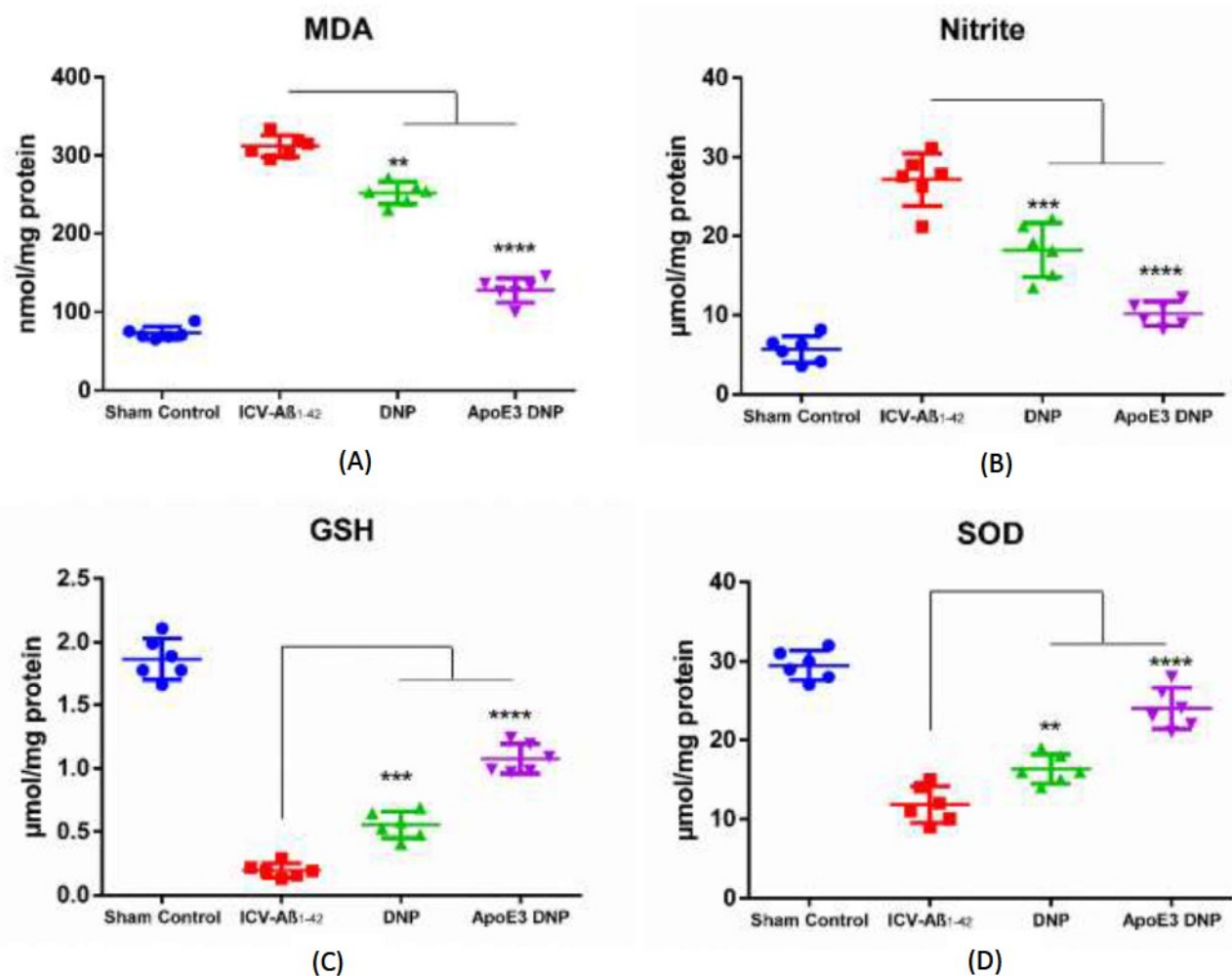


Fig.6.12 Effect of DNP and its formulation on oxidative markers (A) MDA, (B) Nitrite, (C) GSH and (D) SOD, * indicates $p < 0.05$, when compared with disease control

(iii) Estimation of pro-inflammatory cytokines

Studies have been reported that on the infusion of ICV- $A\beta_{1-42}$ in rats elevated the levels of pro-inflammatory cytokines in the hippocampus region. We found that significant upregulation of pro-inflammatory markers TNF- α and IL-6 in case of ICV- $A\beta_{1-42}$ group. On treatment with DNP and D3-NPs decrease in these levels were observed. However, D3-NPs significantly suppressed the neuroinflammation as compared to free drug alone (Fig. 6.13).

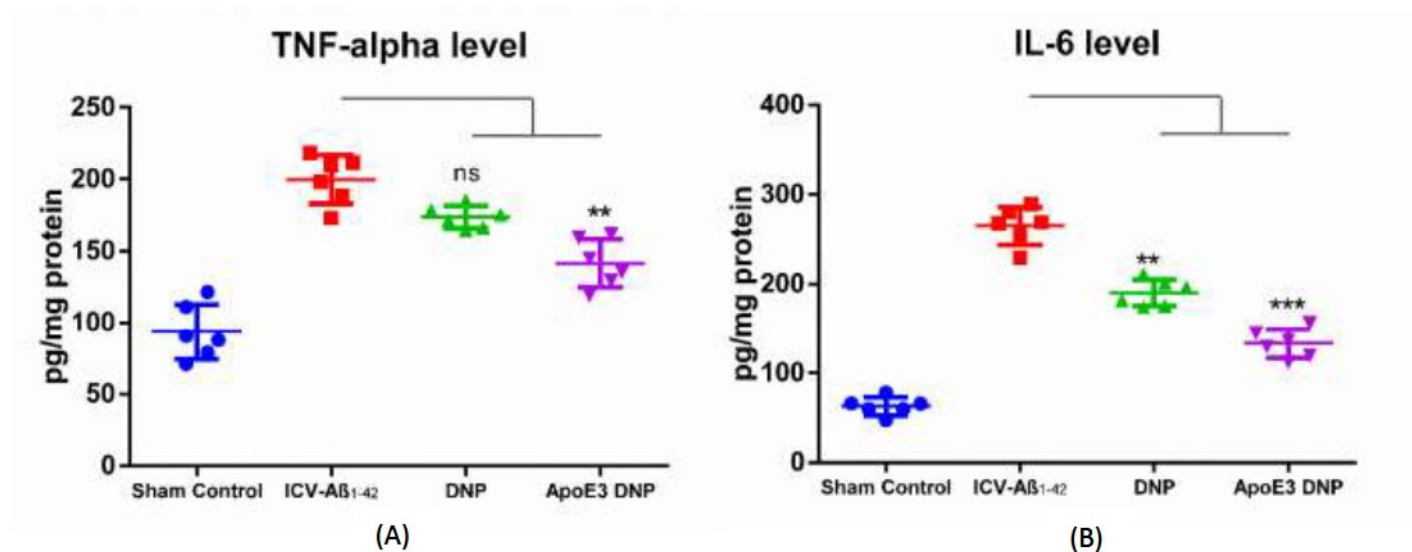


Fig.6.13 Effect of DNP and its formulation on pro-inflammatory markers (A) TNF- α and (B) IL-6, * indicates $p < 0.05$, when compared with disease control

(iv) Estimation of BDNF level

BDNF levels were significantly decreased in ICV-Aβ₁₋₄₂ group than the sham control. When treated with free drug and D3-NPs a significant ameliorate the BDNF levels in ICV-Aβ₁₋₄₂ induced animals. Whereas, D3-NPs resulted in more consistent amelioration of BDNF levels in comparison with free drug alone (Fig. 6.14).

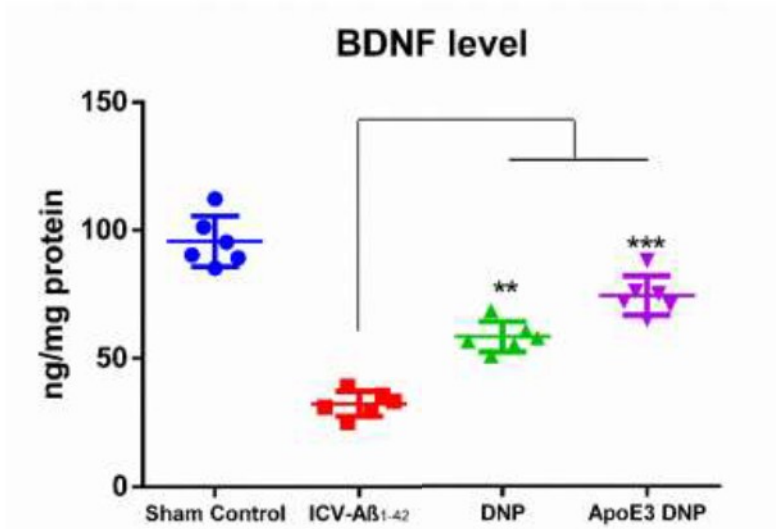


Fig.6.14 Effect of DNP and its formulation on BDNF levels, * indicates $p < 0.05$, when compared with disease control

(v) Estimation of A β ₁₋₄₂ level

It has been well reported that, A β ₁₋₄₂ peptides plays a key role in AD pathogenesis. We have studied the potential influence of D3-NPs over A β ₁₋₄₂ deposition. ICV-A β ₁₋₄₂ administration in rats resulted in significant upregulation in the levels of A β ₁₋₄₂ than the sham control. On treatment with free drug and D3-NPs significantly attenuated the A β ₁₋₄₂ levels in ICV-A β ₁₋₄₂ induced animals. Moreover, D3-NPs exhibited consistent improvement in clearance of A β ₁₋₄₂ levels (Fig. 6.15).

(vi) Estimation of p-tau level

Hyperphosphorylation of tau protein is another characteristic feature in AD pathogenesis. In ICV-A β ₁₋₄₂ administered rats, significant improvement in the p-tau levels was noticed in comparison with the sham control. Whereas on treatment with DNP and D3-NPs, decrease in the levels of p-tau was noticed. Moreover, treatment with D3-NPs showed decreased in p-tau levels in comparison with free drug alone (Fig. 6.15).

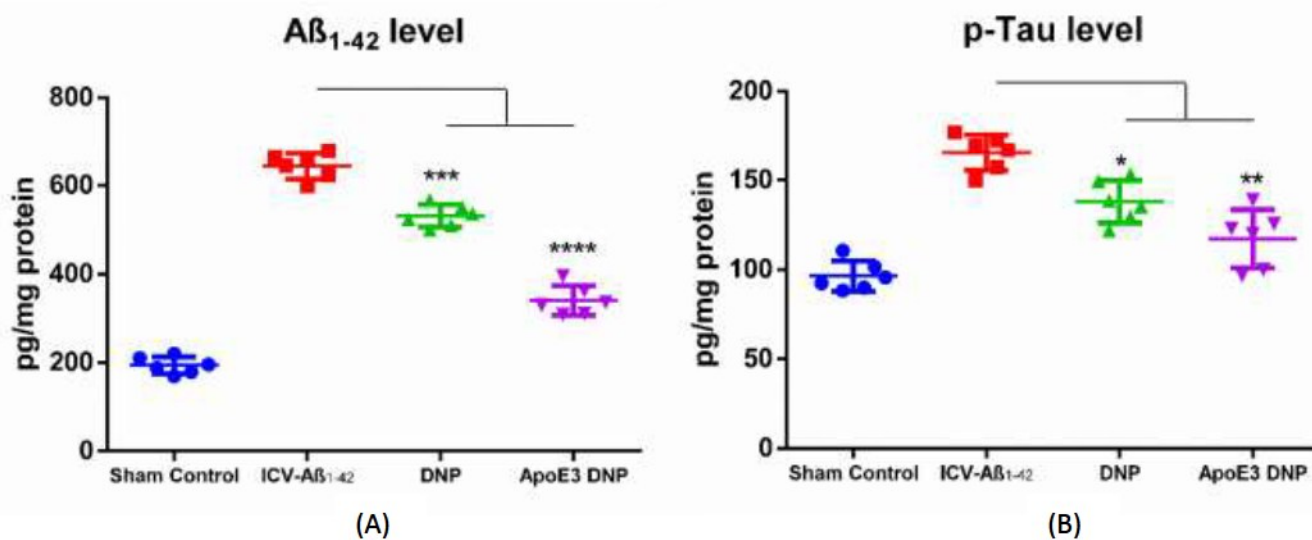


Fig.6.15 Effect of DNP and its formulation on (A) A β ₁₋₄₂ and (B) p-Tau levels, * indicates $p < 0.05$, when compared with disease control

(D) Histopathological studies

We have investigated the ICV- $A\beta_{1-42}$ induced hippocampal neuronal changes such as viable cells, percent damaged neurons, pyknotic neurons by H&E staining. Healthy brain sections from sham control are having spherical nucleus with bulky nucleolus and clear cytoplasm. The histological damage in ICV- $A\beta_{1-42}$ induced animals was identified by pyknotic neurons with dark stained, shrunken with disrupted nucleolus and nucleus. In ICV- $A\beta_{1-42}$ induced animals at DG and CA1 hippocampal regions displayed a significant neuronal damage in comparison with sham control. On treatment with free drug and D3-NPs, a reduced neuronal damage and the percentage of pyknotic neurons was noticed. Although, a significant enhancement was noticed in the group of D3-NPs in comparison with free drug. D3-NPs reduced the hippocampal neuronal loss with improved neuroprotective efficacy and behavioral parameters (Fig. 6.16, 6.17 and 6.18).

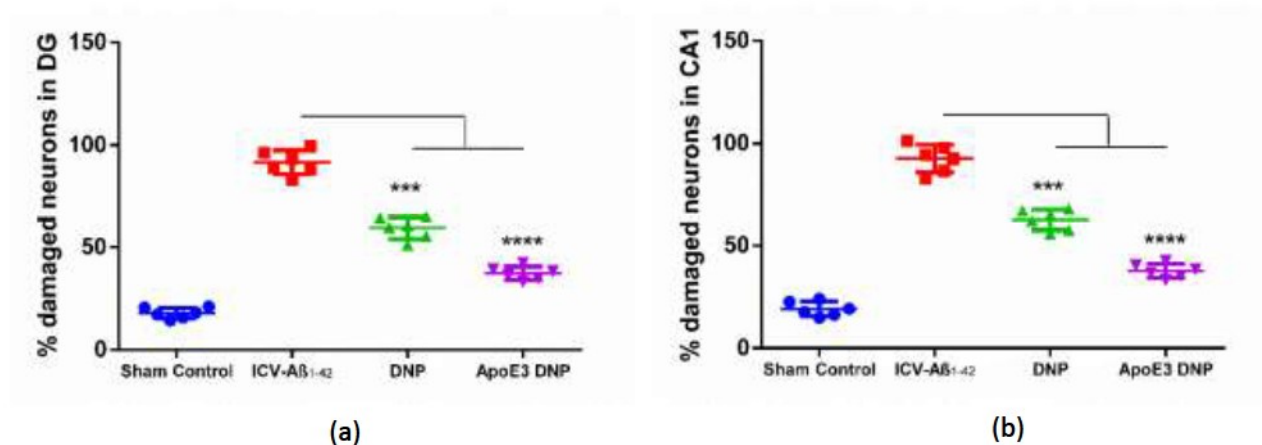


Fig.6.16 Effect of DNP and its formulation on (a) Percent neuronal count in dentate gyrus (DG) region and (c) Percent neuronal count in cornu ammonis (CA1) region

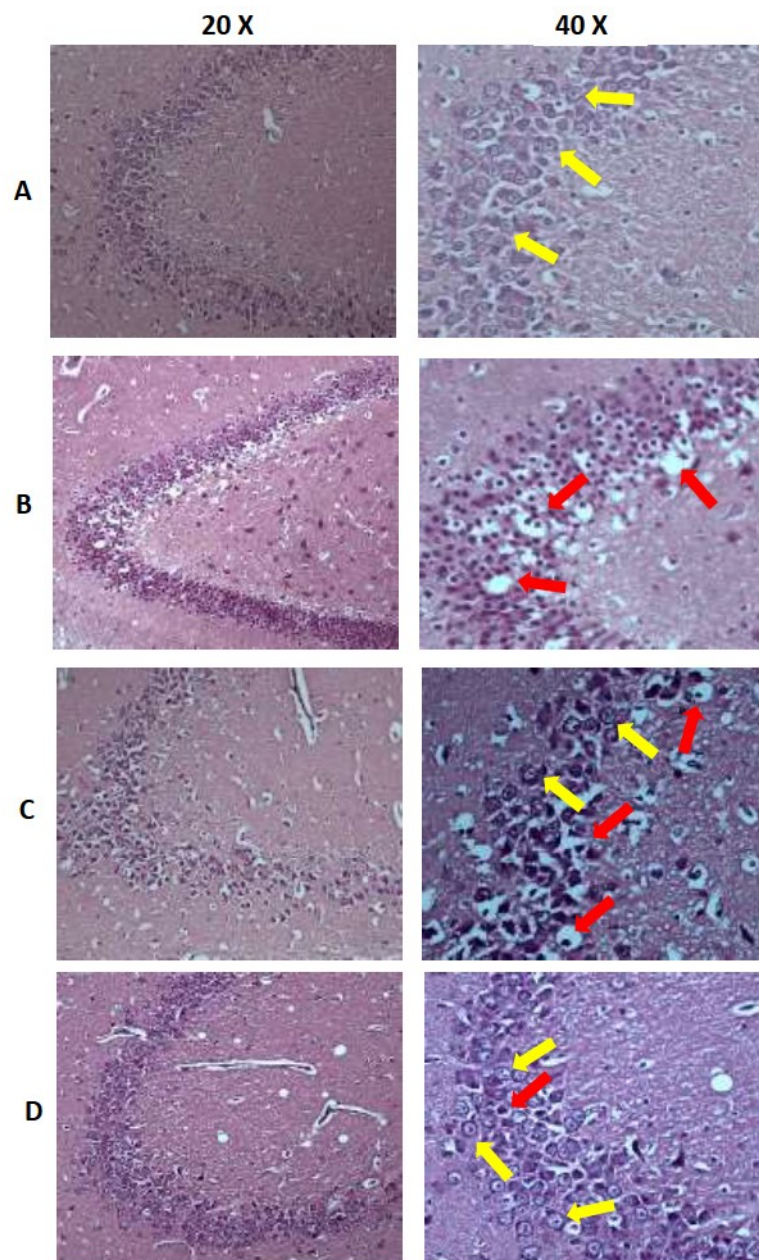


Fig.6.17 Effect of DNP and its formulation on dentate gyrus (DG) region of rat hippocampus, Panel A: Sham control; Panel B: ICV-A β_{1-42} group; Panel C: ICV-A β_{1-42} + DNP; Panel D: ICV-A β_{1-42} + D3-NPs. Red arrows indicate pyknotic neurons and yellow indicates healthy neurons

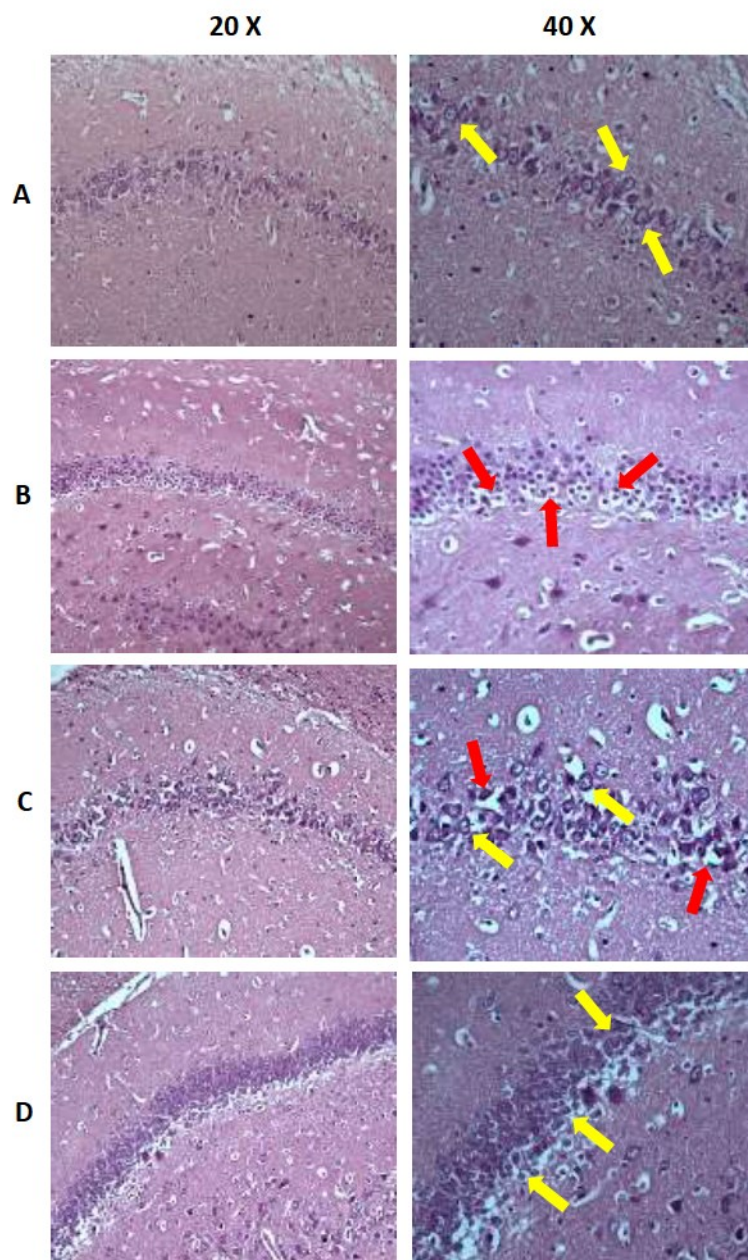


Fig.6.18 Effect of DNP and its formulation on cornu ammonis (CA1) region of rat hippocampus, Panel A: Sham control; Panel B: ICV- $A\beta_{1-42}$ group; Panel C: ICV- $A\beta_{1-42}$ + DNP; Panel D: ICV- $A\beta_{1-42}$ + D3-NPs. Red arrows indicate pyknotic neurons and yellow indicates healthy neurons

Conclusion

The pharmacokinetic, biodistribution and pharmacodynamic studies of free drug and its formulations were performed in rats. Pharmacokinetic studies were carried out for free drug by administering orally and intravenously at a dose of 5 mg/kg and for formulations only oral administration at a same dose. The designed nanoparticles showed significant increment in $AUC_{0-\infty}$ and residence time as it is inferred from the detectable levels of DNP in plasma. Moreover, level A correlation was established using *in vitro* and *in vivo* data. Most importantly our objective was to enhance the brain uptake and it was successfully achieved as the formulations showed significant increase in C_{max} , AUC and MRT compared to the free drug. Biodistribution studies revealed that, D3-NPs has ~5.8 fold ($p < 0.05$) increase in the brain uptake and ~15.30 fold ($p < 0.05$) decrease in brain clearance (Cl) in comparison with the free drug. Although, D1-NPs and D2-NPs also exhibited same trend but the highest brain uptake was observed in D3-NPs due to be presence of surface functionalization with ApoE3 lipoprotein carrier. Moreover, D3-NPs has strong affinity with LDL-R, bind specifically to these receptors and enters brain with the presence of ApoE3. Apart from this, ApoE3 has antiamyloidogenic and antioxidant activities which helps in rapid amyloid beta clearance. Additionally, D3-NPs showed significant decrease in the liver might be because of bypassing of liver and targeting moieties attached over the surface of nanoparticles [15]. On the other hand, significantly reduced concentrations were noticed in the other undesired organs also. Moreover, these finding suggested that the biodistribution studies were in complementary to the systemic pharmacokinetic data as well as cellular uptake studies. ApoE3 coated polymeric nanoparticles have showed better pharmacokinetic parameters and showed a significant increase in DNP concentrations in the brain, that conforms the enhancement of brain uptake [17].

From the pharmacodynamic data it is evident that the D3-NPs have significantly improved behavior and cognition in rats. During MWM task, treatment with D3-NPs attenuated the mean escape latency in ICV- $A\beta_{1-42}$ group. In probe trial also D3-NPs spent significantly more time in the target quadrant representing boosted consolidation of memory. Treatment with D3-NPs in ICV- $A\beta_{1-42}$ group significantly attenuated MDA and nitrite levels, restored GSH level and also showed attenuation of pro-inflammatory markers, TNF- α level and IL-6. Moreover, treatment with D3-NPs showed marked decrease in tau phosphorylation and $A\beta$ levels as compared with untreated

ICV-A β_{1-42} group. Thus, D3-NPs are suitable nano-carrier system for enhancing delivery to the brain and cognition effects.

References

- [1] M. Rowland, T.N. Tozer, *Clinical pharmacokinetics/pharmacodynamics*, Lippincott Williams and Wilkins Philadelphia:, 2005.
- [2] M.W. Jann, K.L. Shirley, G.W. Small, *Clinical pharmacokinetics and pharmacodynamics of cholinesterase inhibitors*, *Clin. Pharmacokinet.* 41 (2002) 719–739.
- [3] K.L. Steinmetz, E.G. Spack, *The basics of preclinical drug development for neurodegenerative disease indications*, in: *BMC Neurol.*, 2009: p. S2.
- [4] F. Alexis, E. Pridgen, L.K. Molnar, O.C. Farokhzad, *Factors affecting the clearance and biodistribution of polymeric nanoparticles*, *Mol. Pharm.* 5 (2008) 505–515.
- [5] D.E. Owens III, N.A. Peppas, *Opsonization, biodistribution, and pharmacokinetics of polymeric nanoparticles*, *Int. J. Pharm.* 307 (2006) 93–102.
- [6] S.M. Moghimi, A.C. Hunter, T.L. Andresen, *Factors controlling nanoparticle pharmacokinetics: an integrated analysis and perspective*, *Annu. Rev. Pharmacol. Toxicol.* 52 (2012) 481–503.
- [7] R.K.R. Rajoli, *Pharmacokinetic Modelling to Study the Biodistribution of Nanoparticles*, in: *Mucosal Deliv. Drugs Biol. Nanoparticles*, Springer, 2020: pp. 247–267.
- [8] M.L. Immordino, F. Dosio, L. Cattel, *Stealth liposomes: review of the basic science, rationale, and clinical applications, existing and potential*, *Int. J. Nanomedicine.* 1 (2006) 297.
- [9] K.H. Wong, M.K. Riaz, Y. Xie, X. Zhang, Q. Liu, H. Chen, Z. Bian, X. Chen, A. Lu, Z. Yang, *Review of current strategies for delivering Alzheimer’s disease drugs across the blood-brain barrier*, *Int. J. Mol. Sci.* 20 (2019) 381.
- [10] D. Gopalan, A. Pandey, N. Udupa, S. Mutalik, *Receptor specific, stimuli responsive and subcellular targeted approaches for effective therapy of Alzheimer: Role of surface engineered nanocarriers*, *J. Control. Release.* 319 (2020) 183–200.
- [11] G. Karthivashan, P. Ganesan, S.-Y. Park, J.-S. Kim, D.-K. Choi, *Therapeutic strategies and nano-drug delivery applications in management of ageing Alzheimer’s disease*, *Drug Deliv.* 25 (2018) 307–320.
- [12] S.K. Sonkusare, C.L. Kaul, P. Ramarao, *Dementia of Alzheimer’s disease and other neurodegenerative disorders—memantine, a new hope*, *Pharmacol. Res.* 51 (2005) 1–17.
- [13] K. Yamaoka, T. Nakagawa, T. Uno, *Application of Akaike’s information criterion (AIC) in*

- the evaluation of linear pharmacokinetic equations, *J. Pharmacokinet. Pharmacodyn.* 6 (1978) 165–175.
- [14] K.V. Krishna, R.N. Saha, G. Singhvi, S.K. Dubey, Pre-clinical pharmacokinetic-pharmacodynamic modelling and biodistribution studies of donepezil hydrochloride by a validated HPLC method, *RSC Adv.* 8 (2018) 24740–24749.
- [15] W. Peng, X. Jiang, Y. Zhu, E. Omari-Siaw, W. Deng, J. Yu, X. Xu, W. Zhang, Oral delivery of capsaicin using MPEG-PCL nanoparticles, *Acta Pharmacol. Sin.* 36 (2015) 139.
- [16] S. Sakore, B. Chakraborty, In vitro-in vivo correlation (IVIVC): a strategic tool in drug development, *J. Bioequiv. Availab. S.* 3 (2011).
- [17] K.V. Krishna, G. Wadhwa, A. Alexander, N. Kanojia, R.N. Saha, R. Kukreti, G. Singhvi, S.K. Dubey, Design and biological evaluation of lipoprotein-based donepezil nanocarrier for enhanced brain uptake through oral delivery, *ACS Chem. Neurosci.* 10 (2019) 4124–4135.
- [18] N. Rajasekar, C. Nath, K. Hanif, R. Shukla, Intranasal insulin improves cerebral blood flow, Nrf-2 expression and BDNF in STZ (ICV)-induced memory impaired rats, *Life Sci.* 173 (2017) 1–10.
- [19] M. Sharma, Y.K. Gupta, Effect of alpha lipoic acid on intracerebroventricular streptozotocin model of cognitive impairment in rats, *Eur. Neuropsychopharmacol.* 13 (2003) 241–247.
- [20] J. Mehla, M. Pahuja, Y.K. Gupta, Streptozotocin-induced sporadic Alzheimer's disease: selection of appropriate dose, *J. Alzheimer's Dis.* 33 (2013) 17–21.
- [21] M. Labak, T. Foniok, D. Kirk, D. Rushforth, B. Tomanek, A. Jasiński, P. Grieb, Metabolic changes in rat brain following intracerebroventricular injections of streptozotocin: a model of sporadic Alzheimer's disease, in: *Brain Edema XIV*, Springer, 2010: pp. 177–181.
- [22] R.G.M. Morris, Morris water maze, *Scholarpedia.* 3 (2008) 6315.
- [23] D. Puzzo, L. Lee, A. Palmeri, G. Calabrese, O. Arancio, Behavioral assays with mouse models of Alzheimer's disease: practical considerations and guidelines, *Biochem. Pharmacol.* 88 (2014) 450–467.
- [24] R. D'Hooge, P.P. De Deyn, Applications of the Morris water maze in the study of learning and memory, *Brain Res. Rev.* 36 (2001) 60–90.
- [25] S.R. Guariglia, K.K. Chadman, Water T-maze: a useful assay for determination of repetitive

- behaviors in mice, *J. Neurosci. Methods*. 220 (2013) 24–29.
- [26] J.D. Bailoo, M.O. Bohlen, D. Wahlsten, The precision of video and photocell tracking systems and the elimination of tracking errors with infrared backlighting, *J. Neurosci. Methods*. 188 (2010) 45–52.
- [27] H.A. Bimonte-Nelson, The Morris maze protocol for rodents, in: *Maz. B.*, Springer, 2015: pp. 441–449.
- [28] C. Zhang, H. Li, R. Han, An open-source video tracking system for mouse locomotor activity analysis, *BMC Res. Notes*. 13 (2020) 48.
- [29] M. Gallagher, R. Burwell, M. Burchinal, Severity of spatial learning impairment in aging: development of a learning index for performance in the Morris water maze., (2015).
- [30] S. Sharma, R. Taliyan, Synergistic effects of GSK-3 β and HDAC inhibitors in intracerebroventricular streptozotocin-induced cognitive deficits in rats, *Naunyn-Schmiedeberg's Arch. Pharmacol.* 388 (2015) 337–349.
- [31] V. Sharma, A. Bala, R. Deshmukh, K.L. Bedi, P.L. Sharma, Neuroprotective effect of RO-20-1724-a phosphodiesterase4 inhibitor against intracerebroventricular streptozotocin induced cognitive deficit and oxidative stress in rats, *Pharmacol. Biochem. Behav.* 101 (2012) 239–245.
- [32] O.H. Lowry, N.J. Rosebrough, A.L. Farr, R.J. Randall, Protein measurement with the Folin phenol reagent, *J. Biol. Chem.* 193 (1951) 265–275.
- [33] G.L. Ellman, K.D. Courtney, V. Andres Jr, R.M. Featherstone, A new and rapid colorimetric determination of acetylcholinesterase activity, *Biochem. Pharmacol.* 7 (1961) 88–95.
- [34] E. Wills, Mechanisms of lipid peroxide formation in animal tissues, *Biochem. J.* 99 (1966) 667.
- [35] H. Ohkawa, N. Ohishi, K. Yagi, Assay for lipid peroxides in animal tissues by thiobarbituric acid reaction, *Anal. Biochem.* 95 (1979) 351–358.
- [36] G.L. Ellman, Tissue sulfhydryl groups, *Arch. Biochem. Biophys.* 82 (1959) 70–77.
- [37] A. Habeeb, Reaction of protein sulfhydryl groups with Ellman's reagent, in: *Methods Enzymol.*, Elsevier, 1972: pp. 457–464.
- [38] L.C. Green, D.A. Wagner, J. Glogowski, P.L. Skipper, J.S. Wishnok, S.R. Tannenbaum, Analysis of nitrate, nitrite, and [^{15}N] nitrate in biological fluids, *Anal. Biochem.* 126 (1982)

- 131–138.
- [39] K.M. Miranda, M.G. Espey, D.A. Wink, A rapid, simple spectrophotometric method for simultaneous detection of nitrate and nitrite, *Nitric Oxide*. 5 (2001) 62–71.
- [40] E.A. Hamed, A.-R.M.A. Meki, N.A.A. El-Mottaleb, Protective effect of green tea on lead-induced oxidative damage in rat's blood and brain tissue homogenates, *J. Physiol. Biochem.* 66 (2010) 143–151.
- [41] H.P. Misra, I. Fridovich, The role of superoxide anion in the autoxidation of epinephrine and a simple assay for superoxide dismutase, *J. Biol. Chem.* 247 (1972) 3170–3175.
- [42] S. Ramagiri, R. Taliyan, Remote limb ischemic post conditioning during early reperfusion alleviates cerebral ischemic reperfusion injury via GSK-3 β /CREB/BDNF pathway, *Eur. J. Pharmacol.* 803 (2017) 84–93.
- [43] R.S. Mulik, J. Mönkkönen, R.O. Juvonen, K.R. Mahadik, A.R. Paradkar, ApoE3 mediated polymeric nanoparticles containing curcumin: apoptosis induced in vitro anticancer activity against neuroblastoma cells, *Int. J. Pharm.* 437 (2012) 29–41.
- [44] R. Morris, Developments of a water-maze procedure for studying spatial learning in the rat, *J. Neurosci. Methods.* 11 (1984) 47–60.



This document was created with the Win2PDF "print to PDF" printer available at <http://www.win2pdf.com>

This version of Win2PDF 10 is for evaluation and non-commercial use only.

This page will not be added after purchasing Win2PDF.

<http://www.win2pdf.com/purchase/>